

Label-free detection of immune complexes with myeloid cells

Zoltán Szittner^{a,b}, Arthur E.H. Bentlage^c, Paolo Rovero^{d,e}, Paola Migliorini^{d,f}, Veronika Lóránd^g, József Prechl^b, Gestur Vidarsson^c

^a Department of Immunology, Eötvös Loránd University, H-1117, Pázmány Péter s. 1/C, Budapest, Hungary

^b Immunology Research Group of the Hungarian Academy of Sciences at Eötvös Loránd University, H-1117, Pázmány Péter s. 1/C, Budapest, Hungary,

^c Department of Experimental Immunohematology, Sanquin Research and Landsteiner Laboratory, Academic Medical Center, University of Amsterdam, 1105 AZ Amsterdam, The Netherlands

^d Toscana Biomarkers Srl, Siena, Italy

^e Department of NeuroFarBa, Section of Pharmaceutical Sciences and Nutraceutics, Laboratory of Peptide and Protein Chemistry and Biology, University of Florence, Via Ugo Schiff 6, 50019 Sesto Fiorentino, Italy

^f Clinical Immunology Unit, Department of Clinical and Experimental Medicine, University of Pisa, Pisa, Italy

^g Department of Rheumatology and Immunology, Clinic Center, PTE, Pécs, Hungary

Short Title: Label-free immune-complex detection by cells

Summary

The aim of this study was to provide proof-of-concept for quantitative and qualitative label-free detection of immune complexes through myeloid cells with imaging surface plasmon resonance. Surface plasmon resonance imaging was first applied to monitor the binding of human sera from healthy and RA patients to immobilised citrullinated RA specific peptide antigens, HCP2 and VCP2. Next, the binding of monocytoïd cell line U937 to the resulting immune complexes on the sensor surface was monitored. As control, binding of U937 was monitored to IgG subclasses simultaneously. Cell response results were compared to results of CCP2 ELISA, clinical RA diagnosis and antigen specific antibody distribution of the samples. Human IgG3 triggered the most pronounced response followed by IgG1 and IgG4, while IgG2 did not result in U937 cell binding. Serum samples obtained from RA patients resulted in significantly increased cell response to VCP2 compared to healthy controls. The strength of cell response towards VCP2-immune complexes showed significant correlation with levels of antigen specific IgA, IgG and IgG3. Cellular responses on VCP2 immune complexes showed significant association with both CCP2-based serological positivity and EULAR criteria-based clinical RA diagnosis. Immunoglobulin-triggered binding of monocytoïd cells can be monitored using a label-free multiplex technology. Since these binding events are presumably initiated by Fc receptors, the system provides a tool for biological detection of autoantibodies with diagnostic value, here exemplified by anti-citrullinated antibodies. This provides added information to antibody levels, as interaction with Fc-receptor-expressing cells are also affected by post-translational modification of the immunoglobulins.

Key words: imaging SPR, IgG, ACPA, Fc Receptor, monocyte

Introduction

Detection of antigen-specific antibody reactivity is of great interest for the diagnosis of various pathogenic conditions. Most commonly this is obtained by measuring antibodies in biological samples, such as from blood serum by ELISA [1] or immunofluorescence based tests [2]. The results obtained represent a simplified view of the immunological reactivity - as only isotype and or IgG subclass of the antigen specific antibody is reported as a biomarker of a given pathological state.

However, the diversity of antigen specific reactivity is much more complex as the magnitude of the effector functions is dependent on the combination of isotypes and subclasses involved and the antibody levels mounted. The antibody glycosylation in the conserved N-linked glycosylation site at position 297 in the Fc portion in IgG and IgE can also be varied and affects binding affinities to Fc-receptors [3-5]. IgG and IgM responses can also lead to activation of the complement system [6], and further opsonisation of innate molecules such as pentraxins [7] can also influence the outcome of the immune response. The resulting immune complex (IC) will eventually lead to differential engagement of Fc- and complement receptors on myeloid effector cells. Thus the final makeup of IC determines the type and magnitude of the resulting inflammatory response [8].

In our previous work we have shown that ICs can be detected through the binding of fluorescently labelled U937 histiocytic lymphoma cells [9] to spotted immunoglobulins and antigens (after serum treatment) on nitrocellulose based microarrays [10]. U937 cells express the IgA receptor (Fc α R), but also the IgG receptors (Fc γ R) Fc γ R1a and Fc γ R1b (CD64 and CD32, respectively) [11]. Their different affinities towards the human IgG subclasses [12] resulted in distinct adhesion profiles depending on the

IgG subclass, which was also affected by complement deposited by these IgG antibodies.

In the current study we report a novel approach where immunological reactivity of serum samples is detected directly and in real-time by the adhesion of immunologically relevant effector cells to immune complexes in a label-free manner using surface plasmon resonance (SPR). Besides the typical measurements such as determination of affinity, specificity and binding kinetics, we and others have shown that cells can also be detected [13-17]. This has been achieved by coupling cellular ligands (e.g. cell surface antigen specific antibodies) covalently onto the sensor and cells are used as analytes, as presented for T- and B-lymphocytes [14] and breast cancer cell lines [17], or by monitoring morphological changes in real-time upon activation [18, 19].

Rheumatoid Arthritis (RA) is an autoimmune disease that is characterized by autoantibody production [20]. These autoantibodies are categorized to two main groups: rheumatoid factors and anti-citrullinated protein antibodies (ACPA). Rheumatoid factors (RF) are usually IgM antibodies directed against the constant region of IgG. Tests determining IgM RF levels have a relatively low specificity (85%), but are routinely used for their sensitivity (69%)[21]. RF positivity was found to be positively correlated with the subsequent onset of RA in a recent prospective study [22] and was reported to have a higher affinity to hypogalactosylated IgG [23]. Moreover ACPA were also found to be hypogalactosylated compared to total IgG1 [24, 25]. ACPA positivity of multiple isotypes precedes the onset of the clinical symptoms in RA[24] and the presence of such autoantibodies is now included in the Classification Criteria of RA [26]. ACPA testing is done routinely with Cyclic Citrullinated Peptide (CCP) ELISA [27]. With this technique isotype distribution can

1
2
3 be monitored as well, however no correlations have been found with disease activity.
4
5 Importantly, ACPA-triggered, FcγR mediated inflammatory cytokine production by
6
7 macrophages has been demonstrated, indicating a pathogenic role for these
8
9 antibodies [28]. Detection of ACPA by SPR Imaging have also been established
10
11 earlier, demonstrating that bio-molecular interactions between citrullinated peptides
12
13 and autoantibodies can be monitored with great precision in real time using this
14
15 technique [29].
16
17

18 In this study we tested whether the ICs formed on sensor surface with RA specific
19
20 antigens trigger adhesion of U937 cells. We then tested if this quantitative information
21
22 on both specific antibodies and their capacity to trigger cellular activation obtained
23
24 simultaneously in a label-free manner yields useful information on the patient's
25
26 clinical state.
27
28
29
30
31
32
33
34
35
36
37
38
39
40
41
42
43
44
45
46
47
48
49
50
51
52
53
54
55
56
57
58
59
60

Materials and Methods

Cell culture

Human premonocytic cell line U937 was cultured in RPMI-1640 medium (Gibco) supplemented with 10% FCS, 2 mM glutamine, penicillin (100 U/ml) and streptomycin (100 µg/ml) and was maintained at 37°C in a humidified atmosphere of 5% carbon dioxide.

Measurement of U937 binding to IgG subclasses and on-sensor formed complexes with IBIS MX96

The IBIS MX96 (Ibis Technologies, Enschede, The Netherlands) surface plasmon resonance imager (SPRi) has several advantages as an array with up to 96, but more conveniently 48, different molecules can be coupled to the sensor surface, monitoring cellular interaction to all of them in parallel in real-time. The microfluidic system of IBIS MX96 with the sensor surface on the bottom facing upwards in the optical imaging chamber enables the application and gravitational sedimentation of cells as demonstrated for red blood cell typing and detection of cell antigens on adherent cells [16, 17]. Human IgG1-4 (Sigma) were spotted in 10 mM acetate buffer, pH 5.4 in replicates to pre-activated Easy2Spot P-type chips (Ssens, Enschede, The Netherlands) using a Continuous Flow Microspotter (Wasatch Microfluidics, Salt Lake City, USA). 100 nM BSA in 10 mM sodium acetate buffer, pH 4 was spotted as negative control and acetate buffer as reference. Multiple Antigenic Peptides (MAPs): Histone derived HCP2 [30], and Epstein-Barr virus derived VCP2 [31] (from Toscana Biomarkers Srl) were spotted at 10 mM and 1 mM spots in replicates in 10 mM acetate buffer, pH 5 and 10 mM MES buffer, pH 6.0 respectively with IgG1 and 3 as positive controls. The sensor was blocked with 1 mg/ml BSA in 10 mM sodium acetate buffer, pH 4 with 0,075% Tween-80 and then with 100 mM ethanolamine,

pH8 with 0.075% Tween-80. Injection of 50 nM anti-kappa-chain specific antibody (mouse anti-human Kappa UNLB, Southern Biotech, clone SB81a) was used to determine equal spotting concentration of the human IgG subclasses, identified as 108 nM for IgG1, 125 nM for IgG2, 100 nM for IgG3 and 148 nM for IgG4. As system and sample buffer PBS with 0.1% BSA (PBS-BSA) was used. All materials including cells and serum samples were diluted in this buffer. For regeneration in between measurements 200 nM H_3PO_4 and 0.5% SDS was used in two cycles to regenerate the sensor surface. The temperature was set to 25°C. Each chip was not used for more than 14 runs.

For testing serum- followed by U937-myeloid cell reactivity to the spotted antigenic peptides, first the baseline (0-300 sec) was set with system buffer. Then 100 μl 1:10 diluted heat-inactivated serum was injected and the sample association took place for 15 minutes under back-and-forth flow. This was followed by the dissociation phase with system buffer, under back and forth flow for 10 minutes. Next U937 cells (200 μl of $2 \times 10^6/\text{ml}$ in PBS-BSA) were injected on the sensor surface and were incubated for 15 minutes after stopping the flow, allowing cells to sediment and bind specific ligands. Changes in angular-shift were recorded to all spots in real time, monitoring both reactivity of sera and cells in corresponding phases of the measurement.

Serum samples

Serum samples from RA patients ($n = 18$) and control serum samples ($n = 5$) were obtained by venopuncture at University of Pécs and at University of Pisa and were stored at -70°C until use. The national ethics committee of Hungary and Italy gave their approval for conducting study with the following contract numbers, respectively: 24973-1/2012/EKU (658/PI/2012.), 45066/2012. RA patients fulfilled the international

Rheumatoid arthritis classification criteria [26]. Serum samples were tested with anti-CCP2 ELISA (InovaDiagnostics, California, USA), according to the manufacturer's instructions. Heat-inactivation was carried out at 56°C for 30 minutes.

Detection of HCP2 and VCP2 specific IgG subclasses in RA samples with ELISA

96 well ELISA plates were coated overnight, 4°C with 5 µg/ml HCP2 and VCP2, diluted in carbonate-bicarbonate buffer pH 9.6 or PBS, respectively. After washing with PBS + 0.05% Tween-20 wells were blocked with PBS + 3% BSA for 1h room temperature (RT), samples were diluted 1:50 in PBS with 1% BSA and 0.05% Tween-20 and were incubated for 3h at on shaker, RT. Subclass specific biotinylated mouse anti-human antibodies (ahIgG1-b and 2b (BD Pharmingen), ahIgG3-b and 4-b (Southern Biotech)) were diluted 1:8000 in PBS-Tween and were incubated for 1h, RT. Biotinylated antibodies were detected with Streptavidin-HRPO (Sigma), diluted 1:5000 in PBS-Tween, 1h, RT. After washing 1% TMB with 0.2% H₂O₂ in TMB buffer was added to each well. After 10 minutes 2N H₂SO₄ was added to each well to stop the reaction. Optical Density was recorded at 450 nm. Control measurements without serum samples were used to determine the background values, background subtracted values were analyzed.

Statistical analysis

Spearman rank correlations were calculated to compare IgG, IgA, IgM and IgG1-4 and U937 and serum association signals on MAPs. Statistical differences in serum binding and cell adhesion during and following incubation of IgG subclasses and MAPs with healthy and RA sera were assessed by pairwise comparisons of relevant

groups using Mann-Whitney U test. To compare the results obtained by cell adhesion to MAPs following serum treatment and results of CCP2 tests and RA diagnosis by physician, Fisher's exact test was used. Statistical tests were considered significant as follows: non-significant (n.s.) - $p \geq 0.05$, * - $p < 0.05$, ** - $p < 0.01$ and *** - $p < 0.001$.

For Peer Review

Results

U937 cells bind to human IgG1, IgG3 and IgG4 but not to IgG2

To simultaneously measure serum responses to antigens and cells we utilized a SPR biosensor system allowing monitoring of up to 48 interactions simultaneously on an array of covalently coupled ligands. While serum reaction can be easily detected by classical SPR, we and others have recently shown the IBIS MX96 system to be capable of red blood cells, platelets and tumour cell detection after gravity sedimentation[16, 17, 32] – but never to deposited ligands. To investigate if U937 cells bind IgG in the IBIS, first we determined the coupling efficiency of each IgG subclass, using antibody against the light chain (anti-kappa monoclonal antibody) shared by all four IgG subclasses. At 100 Response Units (RUs) of each coupled IgG subclass, no significant differences were observed with the anti-kappa IgG suggesting equal coupling. Ten fold dilutions reduced this signal, particularly for IgG2, suggesting alternative configuration on the chip at lower densities (Figure 1A). No anti-kappa signal was detected when IgG were spotted at one RU. We then analysed the interaction between U937 cells with the IgG-coupled chips. After injection of the U937 cells, they were allowed to interact with the sensor surface by sedimentation after stopping the flow (Figure 1B). This resulted in specific interaction of the cells with IgG1, IgG3 and IgG4 compared to BSA, judged by the change in real-time angle-shift. We found that IgG3 was the most effective in triggering cell adherence, IgG1 and IgG4 were roughly half that effective, while IgG2 induced very little or no cell adherence. Interestingly this preference of IgG3 was so pronounced that even at the hundred-fold dilution (~1 nM) some of the spots gave similar response as the 100 RU (Figure 1C). Repeated measurements on a single chip indicated that quantitative measurements could be achieved between all spots within

a single cycle, and between cycles for up to 14 independent runs after repeated use and regenerations (Supplementary Figure 1).

Sera of RA patients lead to myeloid cell detection of VCP2

We next tested if serum-derived reactivity towards antigens can also be detected using myeloid cells as readout. To this end we compared the reactivity of sera from RA patients and normal healthy serum donors (NHS) towards the RA specific citrullinated MAPs: HCP2 and VCP2. As positive controls we spotted hIgG1 and IgG3 at 100 and 10 nM spotting concentrations, and BSA and PBS as negative controls. Incubation of sera showed typical binding resembling antibody-antigen (ligand-receptor) during the association and dissociation phase (left and middle sides of sensograms in Figure 2A, respectively, as summarized in the cartoon in Figure 2B). We noted that sera of RA patients showed significantly elevated serum-reactivity towards IgG1, consistent with increased levels of Rheumatoid factor in these patients (right side Figure 2A, and Figure 2C). Likewise, sera of RA patients showed a significantly increased serum response to HCP2 and VCP2 compared to NHS patients (Figures 2A and 2D). We then introduced the U937 cells, allowing them to interact with the immune complexes deposited on the sensor surface (right half of sensograms in Figure 2A as summarized Figure 2B). U937 cells reacted equally strong to IgG1 and IgG3 equipped control spots treated with NHS and RA sera (Figure 2A and E). Although many NHS showed elevated serum binding to HCP2, these did not result in myeloid U937-binding (Figure 2A, D-F). Importantly, U937 cells reacted significantly stronger with RA-serum-treated VCP2 spots compared to NHS (Figure 2F). The cellular response to HCP2 was not significantly elevated compared to NHS, although RA samples tended to give stronger response. While for HCP2 no correlation was found between levels of serum and cell response, for VCP2, the

cellular response significantly correlated with the level of serum response measured in the same run, showing moderate association (Figure 2G).

VCP2-specific antibody responses correlated with cellular responses

The ability of U937 cells to differentiate among patient sera raised the question whether it was associated to their antigen-specific antibody isotype and subclass composition. For both HCP2 and VCP2, specific antibodies of multiple subclasses were detectable in most of the higher responding samples and the subclasses-levels themselves showed strong correlations with each other (Supplementary Table 1). The same was true for the isotypes, with a strong significant correlation between the antigen specific IgA, IgG and IgM levels (Supplementary Table 2). VCP2 specific serum responses recorded on the IBIS chips correlated significantly with the IgG and IgA levels measured on antigen microarrays (see Supplementary Methods) and with levels of IgG1, IgG3 and IgG4 measured with ELISA, however no correlations were found in case of HCP2 (Supplementary Figure 2).

The antigen specific IgG and IgA levels showed significant correlation with cellular response to VCP2, but not with IgM (Figure 3A). Looking closer at the IgG subclass responses, we found strong significant correlation between IgG3 levels with the U937-reactivity to serum opsonised VCP2-sensor chips (Figure 3B). No significant correlations were found between antibody levels and U937 reactivity for HCP2 (Figure 3A-B).

Cell response on VCP2 shows significant association with CCP2 positivity and RA diagnosis

To evaluate its diagnostic performance, we compared the cellular responses towards the opsonised MAP biosensor with serological and clinical diagnostic RA criteria. For comparison of cellular responses, we categorized samples into positive and negative

sets based on cell response results, using the highest measured cell response value in the NHS group as a cut-off value. We then compared the cellular response to the results of CCP2 ELISA. While VCP2 cell responses showed significant association in both comparisons (Table 1), no significant association was observed for HCP2. By measuring cell responses to serum-opsonised VCP2 chip we could identify 11 out of 12 seropositive (CCP2⁺) and 67% of clinically established RA patients.

Discussion

In this work we examined the application of monocytic cell line U937 to detect immune complexes using label-free SPRi in real time as a potential method to evaluate the clinical relevance of humoral autoantibody formation. We found that immune complexes are formed on relevant RA antigens spotted on the biosensor surface, which are subsequently recognized by myeloid cells. The magnitude of the cellular recognition seemed to be associated with the quality of the deposited antibodies, and be related to clinical signatures in RA.

Detection of immune complexes using cells has several advantages beyond serology. This is because serology alone does not give any information on the quality of the immune response besides isotype or subclass. Any additive qualitative information that affects recognition by effector cells is lost. This can be due to affinity of the antibodies involved, stoichiometry, or antibody Fc-glycosylation – all factors affecting binding to FcγR [5, 33-35].

Using a label-free biosensor method for this task eliminates the need of excessive sample handling in the form of cellular labelling. By applying the antigens on a surface, as opposed to in solution, we potentially mimic surface exposed antigens which change the pathogenic autoantibody and Fc-receptor interactions from low-affinity and low-avidity to high avidity interactions. This mimics the recognition of surface-deposited antibodies - more easily recognized by myeloid cells – which may also occur *in vivo*. However, using SPR for this application has not been widely applied so far due to several challenges not easily solved with most currently available SPR equipment. Here, we utilized a system with reversed optics, allowing for sedimentation of the cells towards the sensor surface, equipped with up to 96

different antigens which can be monitored in parallel. During the process sera and cells are injected serially. After injection of the cells, they are allowed sediment onto the sensor surface, and then interact with molecules opsonised on the sensor surface, allowing adhesion of the cells, registered as change in the angle shift measured by classical SPR methods [16].

First we looked at the cell adhesion to human IgG subclasses and found that the cells recognize and adhere to these molecules presumably through their FcγR. U937 cells express FcγRs: FcγRIIa, and FcγRI[36]. The high affinity FcγRI can bind IgG1, IgG3 and IgG4 but not IgG2. U937 cells expresses the R131 variant of FcγRIIa [37], which binds most efficiently IgG1 and IgG3, slightly better than IgG4, and has minimal reactivity to IgG2 [12, 38]. In addition, U937 cells may express the inhibitory FcγRIIb [39, 40], but this is still controversial [41]. FcγRIIb has the lowest affinity to IgG of all human FcγRs and binds all subclasses except IgG2 [12]. Binding of U937 cells to human IgG subclasses in SPRi measurements followed the pattern of the relative affinity of FcγRs expressed on U937 cells, favouring IgG3 over IgG1 and IgG4 and showing no or little reactivity to IgG2. This is in accordance with our previous results based on nitrocellulose based microarray experiments [10].

Measurement of RA specific reactivity of sera by citrullin-arginin peptide pairs coupled to SPRi sensors have been demonstrated earlier [29], also with HCP2 and VCP2 peptides in a Biacore system [42]. In agreement with those studies, we also found patients sera react to these peptides in our biosensor setup. We then injected U937 cells and allowed them to interact with the opsonised sensor surface without flow. We observed a specific interaction of the U937 cells with the MAPs-sensor spots after opsonisation with reactive sera on-chip. Previous studies investigating anti-keratin antibodies [43], and later ACPA in samples from RA patients revealed

different isotype distribution when measured on different peptides, mostly with high IgG1-levels, frequent IgG4-positivity, but without IgG2 [43-47]. Class-switching is generally thought to develop before the onset of the specific spectra of symptoms characterizing RA[48]. Comparison of ACPA isotypes in samples from RA patients and their healthy relatives showed that unaffected relatives may also have ACPA, most frequently IgG1 and IgA, while a more diverse isotype contribution was characteristic for RA symptoms [49]. The presence of five or more ACPA antibody types and high levels of total IgG anti-CCP2 were associated with more severe disease progression [44]. In general IgM, IgA and the IgG subclasses all seem to contribute to ACPA-mediated clinical symptoms, with the available data suggesting ACPA IgG being the most prominent disease inducer[44, 50, 51]. In agreement with this published literature, it was difficult to pinpoint a single isotype or IgG-subclass promoting the strongest cellular response, as all show underlying secondary correlations. Serum response measured on HCP2 significantly discriminated the RA and NHS group, yet this did not lead to a significant cell response. This may possibly be due to high concentrations of low affinity IgM outcompeting IgG. The deposited IgM would also not be expected to lead to cellular activation as no receptors for IgM have been described on U937 cells. This lack of correlation between serum response and antigen specific IgM possibly results from removal of low-affintiy IgM with thorough washing in our microarray protocol. However, VCP2 specific IgA, IgG and IgG3 levels did show strong correlations with cellular response, mirroring reported clinical associations [46, 52, 53]. For VCP2, serum and cell response showed significant correlation, which was not found for HCP2, suggesting qualitatively distinct set of antibodies recognizing these two antigens. The moderate association in case of VCP2 further supports the notion that cellular response, given a sufficient serum

1
2
3 response, is driven rather by the quality over the quantity of the reacting serum
4
5 components.
6
7

8 The present method shows that interactions of monocytoïd cells with citrullinated
9
10 peptides after incubation with patient sera is strongly associated with the diagnosis of
11
12 RA and CCP positivity. Further development of the presented method, utilizing more
13
14 target peptides and proteins in a single run should help us to determine antigen
15
16 specific immune response in more detail. An added information would be acquired if
17
18 the donors own cells could be used, as the response is also likely to be influenced by
19
20 the polymorphism of FcγRs [38, 54]. Characterizing the effector function-triggered
21
22 cell activation by serum antibodies on different antigens could provide further insight
23
24 into disease state and activity in a personalized manner. In conclusion, this method
25
26 may detect among disease specific antibodies those endowed with a pathogenic
27
28 potential, but further studies on a group of well characterised RA patients will be
29
30 necessary to verify the clinical significance of these findings.
31
32
33
34
35
36
37
38
39
40
41
42
43
44
45
46
47
48
49
50
51
52
53
54
55
56
57
58
59
60

1
2
3
4
5
6
7
8
9
10
11
12
13
14
15
16
17
18
19
20
21
22
23
24
25
26
27
28
29
30
31
32
33
34
35
36
37
38
39
40
41
42
43
44
45
46
47
48
49
50
51
52
53
54
55
56
57
58
59
60

Conflict of Interest

PM and PR are founders of Toscana Biomarkers Srl, the company that owns patent rights on VCP and HCP peptides.

Funding:

This work was supported by the European Union Seventh Framework Programme FP7/2007–2013 under grant agreement [GAPaid-314971, FP7-SME-2012], entitled ‘Genes and proteins for autoimmunity diagnostics’ and OTKA [109683] awarded to JP. ZS was supported by an EFIS-IL Short Term Fellowship.

Peer Review

References

1. Gan SD, Patel KR. Enzyme immunoassay and enzyme-linked immunosorbent assay. *The Journal of investigative dermatology* 2013; **133**:e12.
2. Willitzki A, Hiemann R, Peters V, Sack U, Schierack P, Rodiger S, Anderer U, Conrad K, Bogdanos DP, Reinhold D, Roggenbuck D. New Platform Technology for Comprehensive Serological Diagnostics of Autoimmune Diseases. *Clin Dev Immunol* 2012.
3. Arnold JN, Wormald MR, Sim RB, Rudd PM, Dwek RA. The impact of glycosylation on the biological function and structure of human immunoglobulins. *Annual review of immunology* 2007; **25**:21-50.
4. Kapur R, Kustiawan I, Vestrheim A, Koeleman CA, Visser R, Einarsdottir HK, Porcelijn L, Jackson D, Kumpel B, Deelder AM, Blank D, Skogen B, Killie MK, Michaelsen TE, de Haas M, Rispens T, van der Schoot CE, Wuhrer M, Vidarsson G. A prominent lack of IgG1-Fc fucosylation of platelet alloantibodies in pregnancy. *Blood* 2014; **123**:471-80.
5. Vidarsson G, Dekkers G, Rispens T. IgG subclasses and allotypes: from structure to effector functions. *Frontiers in immunology* 2014; **5**:520.
6. Degn SE, Thiel S. Humoral pattern recognition and the complement system. *Scandinavian journal of immunology* 2013; **78**:181-93.
7. Mantovani A, Valentino S, Gentile S, Inforzato A, Bottazzi B, Garlanda C. The long pentraxin PTX3: a paradigm for humoral pattern recognition molecules. *Annals of the New York Academy of Sciences* 2013; **1285**:1-14.
8. Rojko JL, Evans MG, Price SA, Han B, Waine G, DeWitte M, Haynes J, Freimark B, Martin P, Raymond JT, Evering W, Rebelatto MC, Schenck E, Horvath C. Formation, Clearance, Deposition, Pathogenicity, and Identification of Biopharmaceutical-related Immune Complexes: Review and Case Studies. *Toxicologic pathology* 2014; **42**:725-64.
9. Sundstrom C, Nilsson K. Establishment and characterization of a human histiocytic lymphoma cell line (U-937). *International journal of cancer Journal international du cancer* 1976; **17**:565-77.
10. Szittner Z, Papp K, Sandor N, Bajtay Z, Prechl J. Application of fluorescent monocytes for probing immune complexes on antigen microarrays. *PloS one* 2013; **8**:e72401.
11. Boltz-Nitulescu G, Willheim M, Spittler A, Leutmezer F, Tempfer C, Winkler S. Modulation of IgA, IgE, and IgG Fc receptor expression on human mononuclear phagocytes by 1 alpha,25-dihydroxyvitamin D3 and cytokines. *Journal of leukocyte biology* 1995; **58**:256-62.
12. Bruhns P, Iannascoli B, England P, Mancardi DA, Fernandez N, Jorieux S, Daeron M. Specificity and affinity of human Fc gamma receptors and their polymorphic variants for human IgG subclasses. *Blood* 2009; **113**:3716-25.
13. Yanase Y, Hiragun T, Ishii K, Kawaguchi T, Yanase T, Kawai M, Sakamoto K, Hide M. Surface plasmon resonance for cell-based clinical diagnosis. *Sensors (Basel)* 2014; **14**:4948-59.
14. Suraniti E, Sollier E, Calemczuk R, Livache T, Marche PN, Villiers MB, Roupioz Y. Real-time detection of lymphocytes binding on an antibody chip using SPR imaging. *Lab on a chip* 2007; **7**:1206-8.
15. Quinn JG, O'Kennedy R, Smyth M, Moulds J, Frame T. Detection of blood group antigens utilising immobilised antibodies and surface plasmon resonance. *Journal of immunological methods* 1997; **206**:87-96.
16. Schasfoort RB, Bentlage AE, Stojanovic I, van der Kooi A, van der Schoot E, Terstappen LW, Vidarsson G. Label-free cell profiling. *Analytical biochemistry* 2013; **439**:4-6.
17. Stojanovic I, Schasfoort RB, Terstappen LW. Analysis of cell surface antigens by Surface Plasmon Resonance imaging. *Biosensors & bioelectronics* 2014; **52**:36-43.

18. Yanase Y, Hiragun T, Yanase T, Kawaguchi T, Ishii K, Hide M. Application of SPR imaging sensor for detection of individual living cell reactions and clinical diagnosis of type I allergy. *Allergology international : official journal of the Japanese Society of Allergology* 2013; **62**:163-9.

19. Peterson AW, Halter M, Tona A, Bhadriraju K, Plant AL. Using surface plasmon resonance imaging to probe dynamic interactions between cells and extracellular matrix. *Cytometry Part A : the journal of the International Society for Analytical Cytology* 2010; **77**:895-903.

20. McInnes IB, Schett G. The pathogenesis of rheumatoid arthritis. *The New England journal of medicine* 2011; **365**:2205-19.

21. Nishimura K, Sugiyama D, Kogata Y, Tsuji G, Nakazawa T, Kawano S, Saigo K, Morinobu A, Koshiba M, Kuntz KM, Kamae I, Kumagai S. Meta-analysis: diagnostic accuracy of anti-cyclic citrullinated peptide antibody and rheumatoid factor for rheumatoid arthritis. *Annals of internal medicine* 2007; **146**:797-808.

22. Nielsen SF, Bojesen SE, Schnohr P, Nordestgaard BG. Elevated rheumatoid factor and long term risk of rheumatoid arthritis: a prospective cohort study. *BMJ* 2012; **345**:e5244.

23. Soltys AJ, Hay FC, Bond A, Axford JS, Jones MG, Randen I, Thompson KM, Natvig JB. The binding of synovial tissue-derived human monoclonal immunoglobulin M rheumatoid factor to immunoglobulin G preparations of differing galactose content. *Scandinavian journal of immunology* 1994; **40**:135-43.

24. Willemze A, Trouw LA, Toes RE, Huizinga TW. The influence of ACPA status and characteristics on the course of RA. *Nature reviews Rheumatology* 2012; **8**:144-52.

25. Scherer HU, van der Woude D, Ioan-Facsinay A, el Bannoudi H, Trouw LA, Wang J, Haupl T, Burmester GR, Deelder AM, Huizinga TW, Wuhrer M, Toes RE. Glycan profiling of anti-citrullinated protein antibodies isolated from human serum and synovial fluid. *Arthritis and rheumatism* 2010; **62**:1620-9.

26. Aletaha D, Neogi T, Silman AJ, Funovits J, Felson DT, Bingham CO, 3rd, Birnbaum NS, Burmester GR, Bykerk VP, Cohen MD, Combe B, Costenbader KH, Dougados M, Emery P, Ferraccioli G, Hazes JM, Hobbs K, Huizinga TW, Kavanaugh A, Kay J, Kvien TK, Laing T, Mease P, Menard HA, Moreland LW, Naden RL, Pincus T, Smolen JS, Stanislawski-Biernat E, Symmons D, Tak PP, Upchurch KS, Vencovsky J, Wolfe F, Hawker G. 2010 Rheumatoid arthritis classification criteria: an American College of Rheumatology/European League Against Rheumatism collaborative initiative. *Arthritis and rheumatism* 2010; **62**:2569-81.

27. Pruijn GJ, Wiik A, van Venrooij WJ. The use of citrullinated peptides and proteins for the diagnosis of rheumatoid arthritis. *Arthritis research & therapy* 2010; **12**:203.

28. Clavel C, Nogueira L, Laurent L, Iobagiu C, Vincent C, Sebbag M, Serre G. Induction of macrophage secretion of tumor necrosis factor alpha through Fc gamma receptor IIa engagement by rheumatoid arthritis-specific autoantibodies to citrullinated proteins complexed with fibrinogen. *Arthritis and rheumatism* 2008; **58**:678-88.

29. Lokate AM, Beusink JB, Besselink GA, Pruijn GJ, Schasfoort RB. Biomolecular interaction monitoring of autoantibodies by scanning surface plasmon resonance microarray imaging. *Journal of the American Chemical Society* 2007; **129**:14013-8.

30. Pratesi F, Dioni I, Tommasi C, Alcaro MC, Paolini I, Barbetti F, Boscaro F, Panza F, Puxeddu I, Rovero P, Migliorini P. Antibodies from patients with rheumatoid arthritis target citrullinated histone 4 contained in neutrophils extracellular traps. *Annals of the rheumatic diseases* 2014; **73**:1414-22.

31. Pratesi F, Tommasi C, Anzilotti C, Puxeddu I, Sardano E, Di Colo G, Migliorini P. Antibodies to a new viral citrullinated peptide, VCP2: fine specificity and correlation with anti-cyclic citrullinated peptide (CCP) and anti-VCP1 antibodies. *Clinical and experimental immunology* 2011; **164**:337-45.

32. Kapur R, Heitink-Polle KM, Porcelijn L, Bentlage AE, Bruin MC, Visser R, Roos D, Schasfoort RB, de Haas M, van der Schoot CE, Vidarsson G. C-reactive protein enhances IgG-mediated phagocyte responses and thrombocytopenia. *Blood* 2015; **125**:1793-802.

33. Diebolder CA, Beurskens FJ, de Jong RN, Koning RI, Strumane K, Lindorfer MA, Voorhorst M, Ugurlar D, Rosati S, Heck AJ, van de Winkel JG, Wilson IA, Koster AJ, Taylor RP, Saphire EO, Burton DR, Schuurman J, Gros P, Parren PW. Complement is activated by IgG hexamers assembled at the cell surface. *Science* 2014; **343**:1260-3.
34. Lux A, Yu X, Scanlan CN, Nimmerjahn F. Impact of immune complex size and glycosylation on IgG binding to human FcγR1s. *J Immunol* 2013; **190**:4315-23.
35. Kapur R, Einarsdottir HK, Vidarsson G. IgG-effector functions: "the good, the bad and the ugly". *Immunology letters* 2014; **160**:139-44.
36. Tacke PJ, Batenburg JJ. Monocyte CD64 or CD89 targeting by surfactant protein D/anti-Fc receptor mediates bacterial uptake. *Immunology* 2006; **117**:494-501.
37. Valenzuela NM, Trinh KR, Mulder A, Morrison SL, Reed EF. Monocyte Recruitment by HLA IgG-Activated Endothelium: The Relationship Between IgG Subclass and FcγR1a Polymorphisms. *American journal of transplantation : official journal of the American Society of Transplantation and the American Society of Transplant Surgeons* 2015.
38. Hogarth PM, Pietersz GA. Fc receptor-targeted therapies for the treatment of inflammation, cancer and beyond. *Nature reviews Drug discovery* 2012; **11**:311-31.
39. Valenzuela NM, Mulder A, Reed EF. HLA class I antibodies trigger increased adherence of monocytes to endothelial cells by eliciting an increase in endothelial P-selectin and, depending on subclass, by engaging FcγR1s. *J Immunol* 2013; **190**:6635-50.
40. Tridandapani S, Siefker K, Teillaud JL, Carter JE, Wewers MD, Anderson CL. Regulated expression and inhibitory function of FcγR1b in human monocytic cells. *The Journal of biological chemistry* 2002; **277**:5082-9.
41. Veri MC, Gorlatov S, Li H, Burke S, Johnson S, Stavenhagen J, Stein KE, Bonvini E, Koenig S. Monoclonal antibodies capable of discriminating the human inhibitory FcγR1b (CD32B) from the activating FcγR1a (CD32A): biochemical, biological and functional characterization. *Immunology* 2007; **121**:392-404.
42. Rossi G, Real-Fernandez F, Panza F, Barbetti F, Pratesi F, Rovero P, Migliorini P. Biosensor analysis of anti-citrullinated protein/peptide antibody affinity. *Analytical biochemistry* 2014; **465**:96-101.
43. Vincent C, Serre G, Basile JP, Lestra HC, Girbal E, Sebbag M, Soleilhavoup JP. Subclass distribution of IgG antibodies to the rat oesophagus stratum corneum (so-called anti-keratin antibodies) in rheumatoid arthritis. *Clinical and experimental immunology* 1990; **81**:83-9.
44. van der Woude D, Syversen SW, van der Voort EI, Verpoort KN, Goll GL, van der Linden MP, van der Helm-van Mil AH, van der Heijde DM, Huizinga TW, Kvien TK, Toes RE. The ACPA isotype profile reflects long-term radiographic progression in rheumatoid arthritis. *Annals of the rheumatic diseases* 2010; **69**:1110-6.
45. Chapuy-Regaud S, Nogueira L, Clavel C, Sebbag M, Vincent C, Serre G. IgG subclass distribution of the rheumatoid arthritis-specific autoantibodies to citrullinated fibrin. *Clinical and experimental immunology* 2005; **139**:542-50.
46. Verpoort KN, Jol-van der Zijde CM, Papendrecht-van der Voort EA, Ioan-Facsinay A, Drijfhout JW, van Tol MJ, Breedveld FC, Huizinga TW, Toes RE. Isotype distribution of anti-cyclic citrullinated peptide antibodies in undifferentiated arthritis and rheumatoid arthritis reflects an ongoing immune response. *Arthritis and rheumatism* 2006; **54**:3799-808.
47. Panza F, Pratesi F, Valoriani D, Migliorini P. Immunoglobulin G subclass profile of anticitrullinated peptide antibodies specific for Epstein Barr virus-derived and histone-derived citrullinated peptides. *The Journal of rheumatology* 2014; **41**:407-8.
48. van Venrooij WJ, van Beers JJ, Pruijn GJ. Anti-CCP antibodies: the past, the present and the future. *Nature reviews Rheumatology* 2011; **7**:391-8.
49. Ioan-Facsinay A, Willemze A, Robinson DB, Peschken CA, Markland J, van der Woude D, Elias B, Menard HA, Newkirk M, Fritzler MJ, Toes RE, Huizinga TW, El-Gabalawy HS. Marked differences in fine specificity and isotype usage of the anti-citrullinated protein antibody in health and disease. *Arthritis and rheumatism* 2008; **58**:3000-8.

50. Ossipova E, Cerqueira CF, Reed E, Kharlamova N, Israelsson L, Holmdahl R, Nandakumar KS, Engstrom M, Harre U, Schett G, Catrina AI, Malmstrom V, Sommarin Y, Klareskog L, Jakobsson PJ, Lundberg K. Affinity purified anti-citrullinated protein/peptide antibodies target antigens expressed in the rheumatoid joint. *Arthritis research & therapy* 2014; **16**:R167.

51. Harre U, Georgess D, Bang H, Bozec A, Axmann R, Ossipova E, Jakobsson PJ, Baum W, Nimmerjahn F, Szarka E, Sarmay G, Krumbholz G, Neumann E, Toes R, Scherer HU, Catrina AI, Klareskog L, Jurdic P, Schett G. Induction of osteoclastogenesis and bone loss by human autoantibodies against citrullinated vimentin. *The Journal of clinical investigation* 2012; **122**:1791-802.

52. Shiozawa K, Kawasaki Y, Yamane T, Yoshihara R, Tanaka Y, Uto K, Shiozawa S. Anticitrullinated protein antibody, but not its titer, is a predictor of radiographic progression and disease activity in rheumatoid arthritis. *The Journal of rheumatology* 2012; **39**:694-700.

53. Demoruelle MK, Deane K. Antibodies to citrullinated protein antigens (ACPAs): clinical and pathophysiologic significance. *Current rheumatology reports* 2011; **13**:421-30.

54. Li X, Gibson AW, Kimberly RP. Human FcR polymorphism and disease. *Current topics in microbiology and immunology* 2014; **382**:275-302.

Figure Legends

Figure 1. U937 cells bind efficiently to human IgG1, IgG3 and IgG4, not IgG2.

(A) IgG subclasses, coupled equally, detected with kappa chain specific antibody. (B) Representative sensogram of IgG subclasses detected with U937 cells. (C) Cell binding expressed as percentage of the highest signal in each cycle. Data in (A and C) shows the mean of three replicate runs with three spots per run. Resonance Unit values shown were recorded in the last 10 seconds of the 15 minute incubation, marked with the dotted frame in (B). Bars represent means with error bars showing Standard Deviation.

Figure 2. Comparison of NHS and RA sera reactivity towards IgG, MAPs, and subsequent recognition by U937 cells.

(A) Representative sensograms recorded for NHS and RA samples, on various ligands, showing phases of the measurement (depicted in (B)), with dashed frames indicating the response values evaluated. (C) Results of serum association measured on IgG1 and IgG3, and (D) MAPs: HCP2 and VCP2, and (E-F) the following cell binding response on these ligands are shown. Symbols in (C-F) mark the mean RU unit obtained on the ligand subtracted by PBS background. Statistical significance (C-F) was calculated by Mann-Whitney U test. (G) Comparison of serum and cell binding response on MAPs, here Spearman's rank correlation coefficients (r) were calculated.

Figure 3. Immunoglobulin levels against citrullinated peptides correlate with U937 responses in RA patients.

(A) HCP2 and VCP2 specific IgA, IgG, IgM measured by microarrays and (B) IgG subclasses as determined by ELISA from RA samples were compared to cell response values obtained from the biosensor experiments measured on the same antigens. Symbols represent the mean of

1
2
3
4
5
6
7
8
9
10
11
12
13
14
15
16
17
18
19
20
21
22
23
24
25
26
27
28
29
30
31
32
33
34
35
36
37
38
39
40
41
42
43
44
45
46
47
48
49
50
51
52
53
54
55
56
57
58
59
60

replicate measurements after subtraction of background values. Spearman's rank correlation coefficients (r) were calculated to evaluate the correlations.

For Peer Review

		U937 cell response			
		VCP2 10 mM		HCP2 1 mM	
		+	-	+	-
CCP2	+	11	2	5	8
	-	1	9	2	8
		p=0.0006, ***		p=0.4050, n.s.	
RA	+	12	6	7	11
	-	0	5	0	5
		p=0.0137, *		p=0.2719, n.s.	

Table 1. RA diagnosis and CCP2 positivity shows association with cellular response against VCP2. Diagnostic performance of cell binding response measured on MAPs after serum incubation with NHS or RA samples were compared to CCP2 tests and RA diagnosis. Results are summarized as a contingency table, separately for comparison with CCP2 test and RA diagnosis results. To assess the associations Fisher's exact test was calculated.

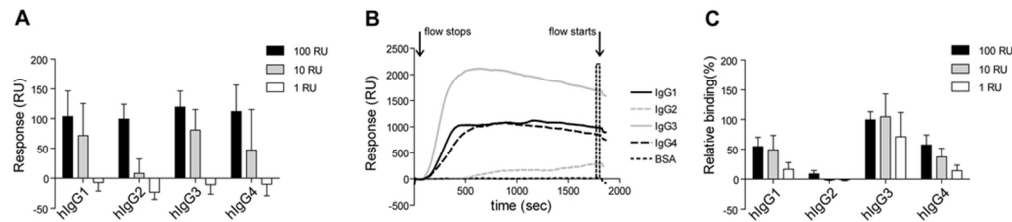


Figure 1. U937 cells bind efficiently to human IgG1, IgG3 and IgG4, not IgG2. (A) IgG subclasses, coupled equally, detected with kappa chain specific antibody. (B) Representative sensogram of IgG subclasses detected with U937 cells. (C) Cell binding expressed as percentage of the highest signal in each cycle. Data in (A and C) shows the mean of three replicate runs with three spots per run. Resonance Unit values shown were recorded in the last 10 seconds of the 15 minute incubation, marked with the dotted frame in (B). Bars represent means with error bars showing Standard Deviation.

43x9mm (600 x 600 DPI)

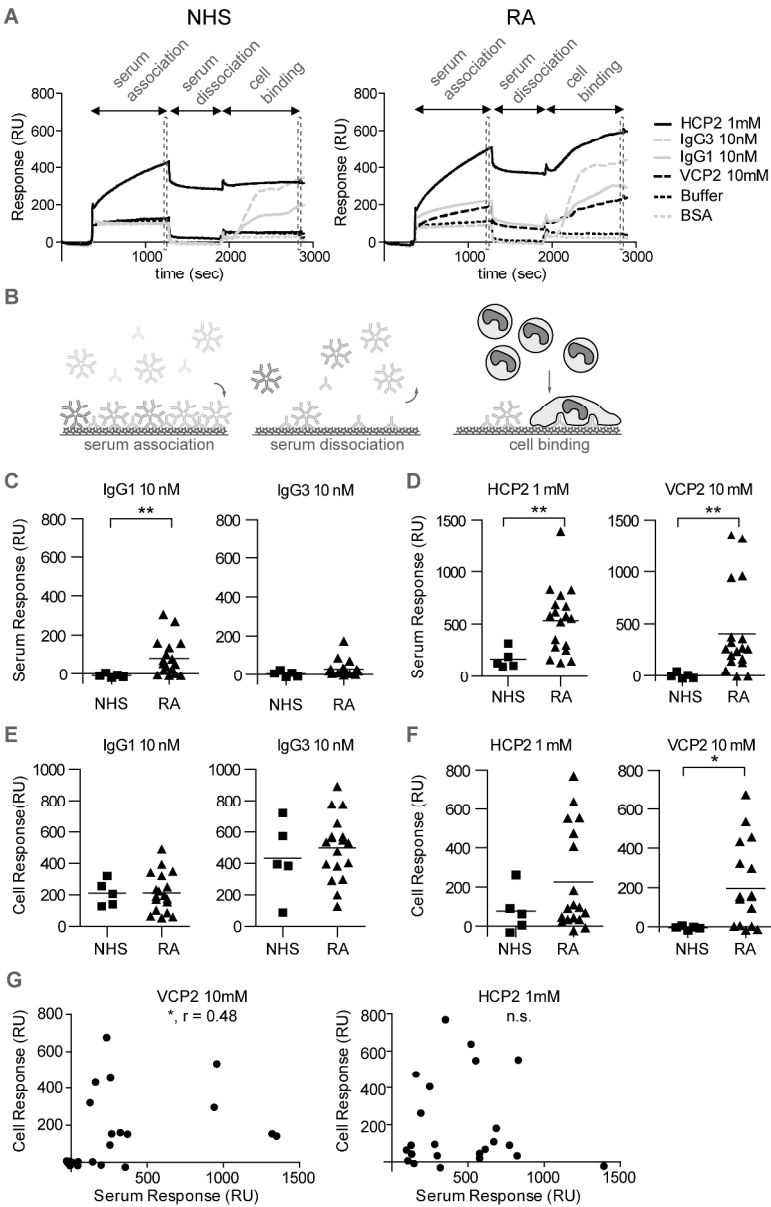


Figure 2. Comparison of NHS and RA sera reactivity towards IgG, MAPs, and subsequent recognition by U937 cells. (A) Representative sensograms recorded for NHS and RA samples, on various ligands, showing phases of the measurement (depicted in (B)), with dashed frames indicating the response values evaluated. (C) Results of serum association measured on IgG1 and IgG3, and (D) MAPs: HCP2 and VCP2, and (E-F) the following cell binding response on these ligands are shown. Symbols in (C-F) mark the mean RU unit obtained on the ligand subtracted by PBS background. Statistical significance (C-F) was calculated by Mann-Whitney U test. (G) Comparison of serum and cell binding response on MAPs, here Spearman's rank correlation coefficients (r) were calculated.

159x247mm (600 x 600 DPI)

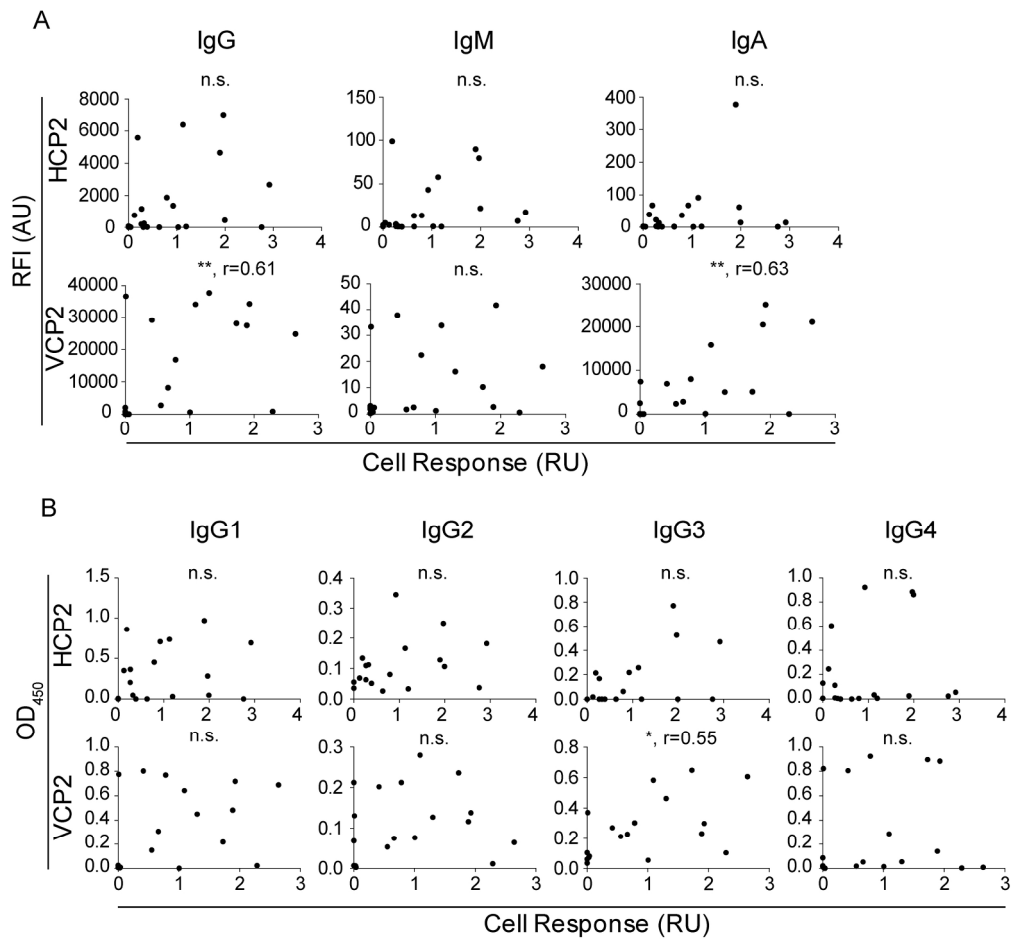
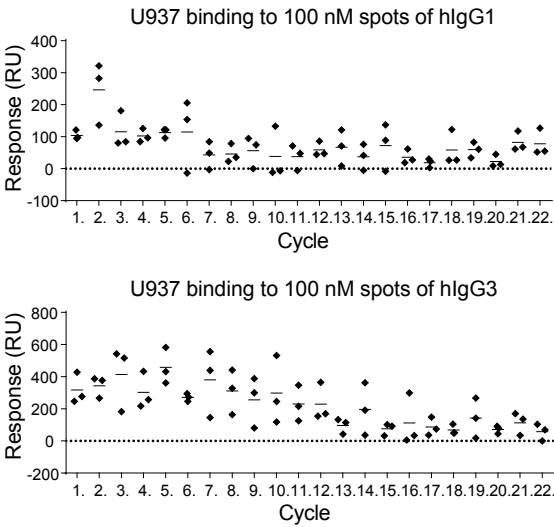


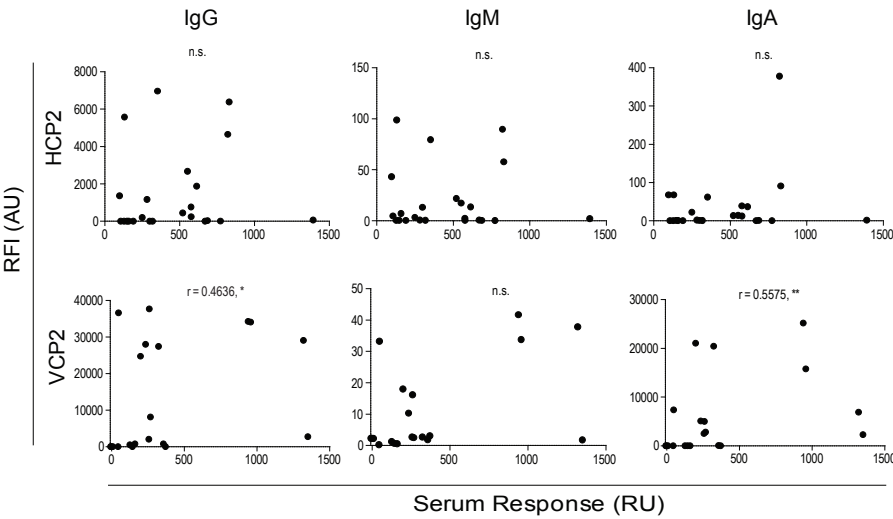
Figure 3. Immunoglobulin levels against citrullinated peptides correlate with U937 responses in RA patients. (A) HCP2 and VCP2 specific IgA, IgG, IgM measured by microarrays and (B) IgG subclasses as determined by ELISA from RA samples were compared to cell response values obtained from the biosensor experiments measured on the same antigens. Symbols represent the mean of replicate measurements after subtraction of background values. Spearman's rank correlation coefficients (r) were calculated to evaluate the correlations.

104x97mm (600 x 600 DPI)

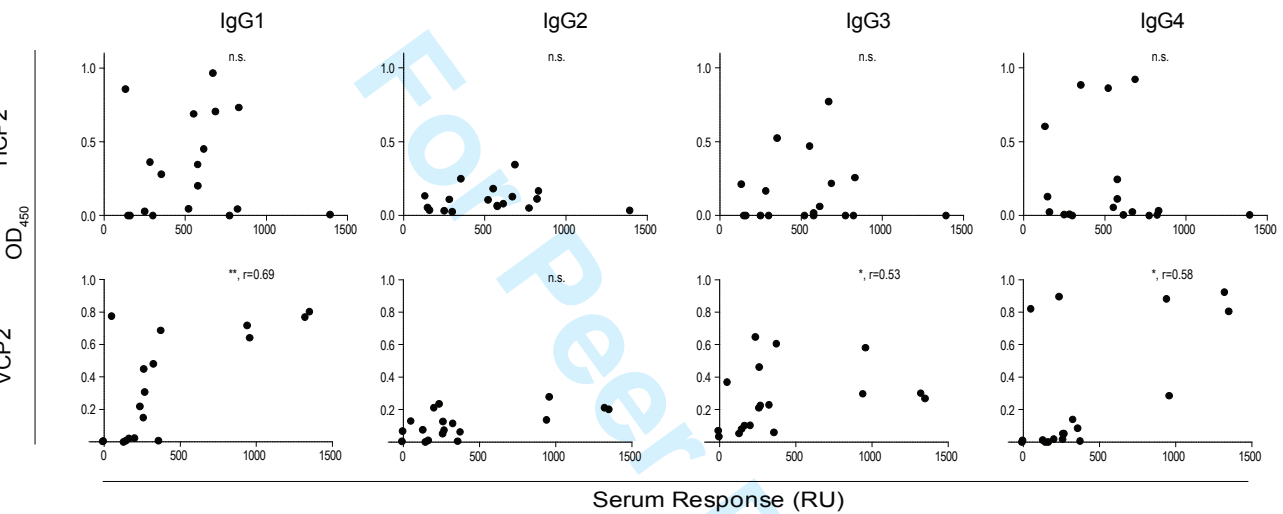


Supplementary Figure 1. Repeated measurements of hIgG1 and hIgG3 with U937 cells. Cell adherence to triplicates of 100 nM spots of IgG1 and IgG3 was recorded in 22 cycles on the same sensor after each other. Each symbol shows results of a single measurement in a cycle, and bars mark the mean of the triplicates. Response expressed in Resonance Units (RU).

A



B



Supplementary Figure 2. Correlation of antigen specific immunoglobulin levels with serum response on MAPs: HCP2 and VCP2. (A) Comparison of antigen specific antibody levels measured by antigen microarray for IgG, IgA and IgM and (B) by ELISA for IgG subclasses with serum association response on MAPs. Spearman's rank correlation coefficients (r) were considered significant as follows: * - $p < 0.05$, ** - $p < 0.01$. n.s. - non significant. RU – response unit, RFI - Relative Fluorescent Intensity, AU - Arbitrary Unit

	IgG1	IgG2	IgG3	IgG4
IgG1	VCP2	r = 0.60 p = 0.00864	r = 0.79 p = 0.00011	r = 0.69 p = 0.00138
IgG2	r = 0.79 p = 0.00008		r = 0.64 p = 0.00464	r = 0.80 p = 0.00008
IgG3	r = 0.86 p = 0.00001	r = 0.83 p = 0.00002		r = 0.60 p = 0.00825
IgG4	r = 0.45 p = 0.06407	r = 0.60 p = 0.00793	r = 0.44 p = 0.07069	HCP2

Supplementary Table 1. Correlation of antigen specific IgG subclass levels of RA serum samples, measured on HCP2 and VCP2. Antigen specific IgG1-4 subclass levels were determined by ELISA. Spearman's rank correlation coefficients(r) are shown in each cell with the row and column headers indicating the compared subclasses for VCP2 in dark gray, and in light gray for HCP2. Correlations were considered significant at p < 0.05.

	IgG	IgA	IgM
IgG	VCP2	$r = 0.75$ $p = 0.00004$	$r = 0.83$ $p < 0.00001$
IgA	$r = 0.72$ $p = 0.00011$		$r = 0.77$ $p = 0.00002$
IgM	$r = 0.89$ $p < 0.00001$	$r = 0.79$ $p = 0.00001$	HCP2

Supplementary Table 2. Correlation of antigen specific IgG, IgM and IgA levels of RA serum samples, measured on HCP2 and VCP2. Antigen specific levels of IgA, IgG and IgM of the samples were determined by antigen microarray. Spearman's rank correlation coefficients(r) are shown in each cell with the row and column headers indicating the compared isotypes for VCP2 in dark gray, and in light gray for HCP2. Correlations were considered significant at $p < 0.05$.